The Cytochrome P450 Enzyme CYP96A15 Is the Midchain Alkane Hydroxylase Responsible for Formation of Secondary Alcohols and Ketones in Stem Cuticular Wax of Arabidopsis[1][W][OA]

Stephen Greer, Miao Wen, David Bird[2], Xuemin Wu, Lacey Samuels, Ljerka Kunst, and Reinhard Jetter*

Department of Botany (S.G., D.B., X.W., L.S., L.K., R.J.) and Department of Chemistry (M.W., R.J.), University of British Columbia, Vancouver, British Columbia, Canada V6T 1Z1

Most aerial surfaces of plants are covered by cuticular wax that is synthesized in epidermal cells. The wax mixture on the inflorescence stems of Arabidopsis (*Arabidopsis thaliana*) is dominated by alkanes, secondary alcohols, and ketones, all thought to be formed sequentially in the decarbonylation pathway of wax biosynthesis. Here, we used a reverse-genetic approach to identify a cytochrome P450 enzyme (CYP96A15) involved in wax biosynthesis and characterized it as a midchain alkane hydroxylase (MAH1). Stem wax of T-DNA insertional mutant alleles was found to be devoid of secondary alcohols and ketones (*mah1-1*) or to contain much lower levels of these components (*mah1-2* and *mah1-3*) than wild type. All mutant lines also had increased alkane amounts, partially or fully compensating for the loss of other compound classes. In spite of the chemical variation between mutant and wild-type waxes, there were no discernible differences in the epicuticular wax crystals on the stem surfaces. Mutant stem wax phenotypes could be partially rescued by expression of wild-type *MAH1* under the control of the native promoter as well as the cauliflower mosaic virus 35S promoter. Cauliflower mosaic virus 35S-driven overexpression of *MAH1* led to ectopic accumulation of secondary alcohols and ketones in Arabidopsis leaf wax, where only traces of these compounds are found in the wild type. The newly formed leaf alcohols and ketones had midchain functional groups on or next to the central carbon, thus matching those compounds in wild-type stem wax. Taken together, mutant analyses and ectopic expression of MAH1 in leaves suggest that this enzyme can catalyze the hydroxylation reaction leading from alkanes to secondary alcohols and possibly also a second hydroxylation leading to the corresponding ketones. MAH1 expression was largely restricted to the expanding regions of the inflorescence stems, specifically to the epidermal pavement cells, but not in trichomes and guard cells. MAH1-green fluorescent protein fusion proteins localized to the endoplasmic reticulum, providing evidence that both intermediate and final products of the decarbonylation pathway are generated in this subcellular compartment and must subsequently be delivered to the plasma membrane for export toward the cuticle.

Above-ground epidermal surfaces of vascular plants are covered by a lipophilic layer known as the cuticle. The cuticle performs physiological, ecological, and developmental roles as a barrier: limiting nonstomatal transpiration (Burghardt and Riederer, 2006), minimizing the adhesion of dust, pollen, and spores (Barthlott and Neinhuis, 1997), protecting tissues from UV radiation (Krauss et al., 1997; Solovchenko and Merzlyak, 2003; Pfündel et al., 2006), mediating biotic interactions with microbes (Carver and Gurr, 2006; Leveau, 2006) as well as insects (Eigenbrode and Espelie, 1995; Müller, 2006), and preventing deleterious fusions between different plant organs (Nawrath, 2006).

Plant cuticles are composed of the fatty acid polyester cutin as well as complex mixtures of very-long-chain (VLC) aliphatic lipids, which form the component known as cuticular wax. Wax that is localized within the cutin matrix is designated intracuticular wax, whereas wax that is deposited as a film or as microcrystals on the outer surface of the cutin polymer is known as epicuticular wax (Jeffree, 2006). Cuticular waxes contain species-characteristic compound classes and chain length patterns (Jetter et al., 2006). The cuticular wax mixture of Arabidopsis (*Arabidopsis thaliana*) leaves consists of VLC alkanes, aldehydes, fatty acids, primary alcohols, corresponding alkyl esters, and small amounts of triterpenoids; the wax on inflorescence stems, although similar, contains high amounts of secondary alcohol and ketone constituents (Rashotte et al., 1997). In fact, alkanes, secondary alcohols, and ketones comprise 80% to 90% of total Arabidopsis stem wax (Rashotte et al., 1997) and it has been postulated that all three compounds are involved

[1] This work was supported by the Natural Sciences and Engineering Research Council of Canada (Special Research Opportunity grant to L.S., L.K., and R.J.), the Canadian Foundation for Innovation, and the Canadian Research Chairs program.

[2] Present address: Department of Biological Sciences, University of Manitoba, Winnipeg, Manitoba, Canada R3T 2N2.

* Corresponding author; e-mail jetter@interchange.ubc.ca.

The author responsible for distribution of materials integral to the findings presented in this article in accordance with the policy described in the Instructions for Authors (www.plantphysiol.org) is: Reinhard Jetter (jetter@interchange.ubc.ca).

[W] The online version of this article contains Web-only data.

[OA] Open Access articles can be viewed online without a subscription.

www.plantphysiol.org/cgi/doi/10.1104/pp.107.107300

in forming the epicuticular wax crystals found on stem surfaces (Rashotte and Feldmann, 1998; Jetter et al., 2006).

Cuticular wax components are formed by elongation of saturated fatty acyl chains and their modification either by the acyl-reduction pathway, yielding primary alcohols and esters, or by the decarbonylation pathway, leading to aldehydes, alkanes, secondary alcohols, and ketones (Fig. 1; Kunst et al., 2006). Forward-genetic approaches have successfully identified some of the genes involved in plant wax biosynthesis from several plant species. For example, visual screenings of mutagenized Arabidopsis populations have yielded a set of 21 *eceriferum* (*cer*) mutants with characteristic changes in the composition of inflorescence stem wax (Koornneef et al., 1989; McNevin et al., 1993). Some of the genes mutated in these *cer* lines have been cloned and characterized, including those coding for the ketoacyl-CoA synthase *CER6* (Millar et al., 1999; Fiebig et al., 2000; Hooker et al., 2002) and the enoyl-CoA reductase *CER10* (Zheng et al., 2005) involved in fatty acid elongation, as well as the fatty acyl-CoA reductase *CER4* that is responsible for primary alcohol synthesis (Rowland et al., 2006). However, not a single step in the decarbonylation pathway has been confirmed through the identification, cloning, and characterization of the predicted enzyme. A few Arabidopsis genes causing mutant wax phenotypes have been putatively linked to early steps in the decarbonylation pathway; among them, *CER1* and *CER3* have been cloned (Aarts et al., 1995; Rowland et al., 2007), but their biochemical functions are still not established.

The last two steps in the decarbonylation pathway are thought to proceed by consecutive oxidation reactions first leading from alkanes to secondary alcohols, and then from secondary alcohols to ketones (Kunst et al., 2006). The biosynthetic link between these three compound classes was first substantiated by biochemical data showing that both alkanes and secondary alcohols can be transformed into ketones in *Brassica oleracea* leaf disc assays (Kolattukudy and Liu, 1970; Kolattukudy et al., 1971, 1973). Based on these findings, it was postulated that alkane hydroxylation and subsequent alcohol oxidation steps are catalyzed by one or two mixed-function oxidases. Further indirect evidence for this reaction sequence came from Arabidopsis

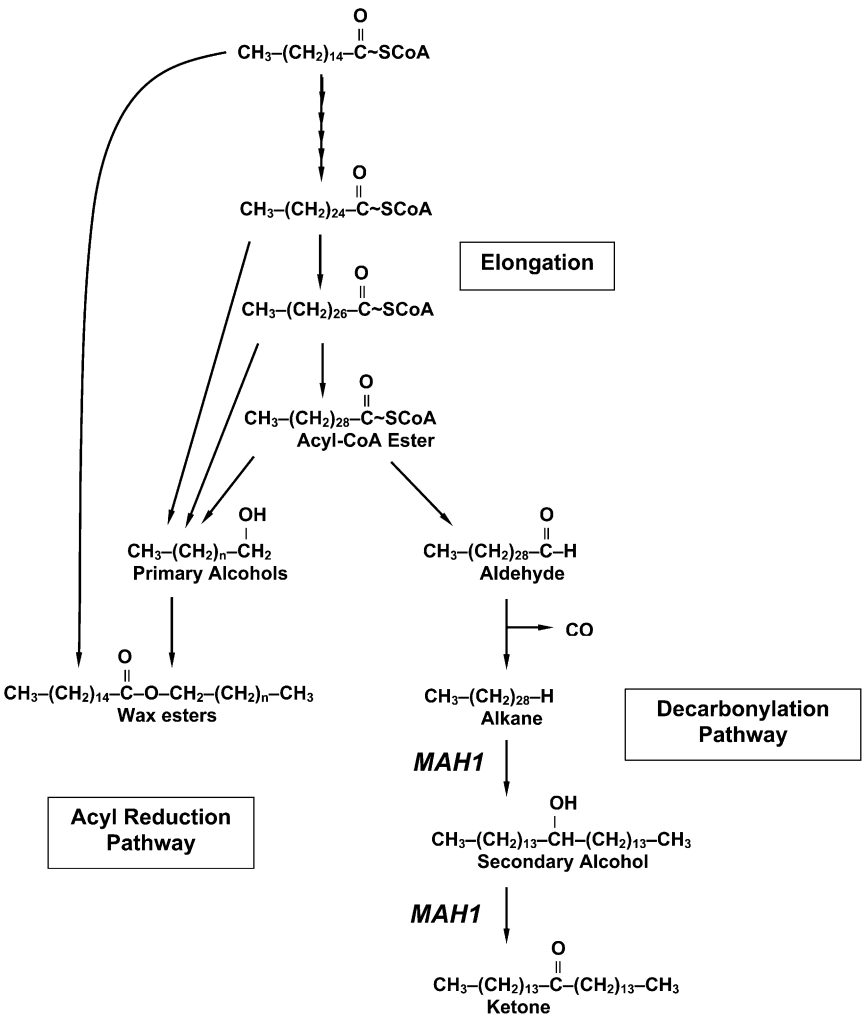

Figure 1. Biosynthetic pathways leading to Arabidopsis cuticular wax components. The acyl reduction pathway yields primary alcohols with even carbon numbers as well as the corresponding wax esters. The decarbonylation pathway leads to the formation of alkanes, secondary alcohols, and ketones with odd carbon numbers. In the decarbonylation pathway, only the reactions modifying 30:0 acyl CoA are shown to illustrate the formation of products with prevalent chain lengths. The proposed action of MAH1 in the decarbonylation pathway is indicated.

studies in which deficiencies in alkanes were correlated with a lack of secondary alcohols and ketones (Millar et al., 1999; Chen et al., 2005); also, *cer20* mutants were reported to have reduced levels of secondary alcohols and ketones, but not alkanes (Rashotte et al., 2001), suggesting that the defective gene product is involved in the alkane hydroxylation step, or possibly also in secondary alcohol oxidation. Unfortunately, no genes or enzymes involved in the process have been identified to date, and therefore the formation of these major compound classes of Arabidopsis wax remain to be investigated on the molecular level.

In the current project, we complemented the previous forward-genetic experiments with a reverse-genetic approach to identify genes responsible for ketone formation in Arabidopsis stems. Prime candidates for the mixed-function oxidases (or monooxygenases) were expected to be in the family of cytochrome P450-dependent enzymes because prior studies had delineated roles for cytochrome P450 oxidation of various lipophilic plant products. Examples include hydroxylation steps in the biosynthesis of terpenoids (Kim et al., 2005; Morikawa et al., 2006; Mau and Croteau, 2006), alkaloids (Collu et al., 2001, 2002), and phenolics (Whitbred and Schuler, 2000; Ehlting et al., 2006). Most notably, cytochrome P450 enzymes have recently also been shown to be involved in the synthesis of cutin monomers by hydroxylating methyl groups at the ω-chain terminus of fatty acids (for review, see Kandel et al., 2006). It stands to reason, then, that a cytochrome P450 enzyme could also be involved in the hydroxylation of alkanes during wax biosynthesis.

The Arabidopsis genome contains 272 cytochrome P450 genes (including 26 pseudogenes; Rhee et al., 2003; Wortman et al., 2003) of which 33 have been grouped together in the *CYP86* clan of non-A-type P450s, which include the subfamilies *CYP86*, *CYP94*, *CYP96*, and *CYP704* (Durst and Nelson, 1995; Nelson et al., 2004). Members from this clan have previously been shown to be involved in the hydroxylation reactions of fatty acyl-derived substrates (Kahn et al., 2001; Wellesen et al., 2001; Werck-Reichhart et al., 2002) and therefore genes within this clan may be regarded as candidates for cuticle biosynthetic enzymes. To further narrow the choice of gene candidates, expression data have to be taken into account. In particular, a recent microarray experiment revealed the genes up-regulated in epidermal cells in stem regions of active wax synthesis and secretion (Suh et al., 2005). A cytochrome P450 gene (*CYP96A15*, At1g57750) with currently unknown function showed 2- to 3-fold up-regulation in the stem epidermis when compared with total stem tissue and we speculated that it may encode the mixed-function oxidase responsible for formation of secondary alcohols and/or ketones found in Arabidopsis stem wax. To test this hypothesis, we performed experiments addressing the following questions: Is this gene involved in the decarbonylation pathway of wax biosynthesis? Can the corresponding gene product catalyze the oxidation from alkanes to secondary alcohols and/or the oxidation from secondary alcohols to ketones? Is this the sole enzyme involved in production of secondary alcohols and ketones or are there other related enzymes? Where in Arabidopsis stem epidermal cells is the enzyme localized?

RESULTS

To investigate whether *CYP96A15* (At1g57750) codes for an enzyme in the decarbonylation pathway catalyzing the cuticular wax secondary alcohols and ketones, three sets of experiments were carried out. First, the wax composition and load of selected T-DNA insertional mutant lines was assessed. Second, ectopic expression of the gene was employed to determine its biochemical function. Finally, gene expression patterns and subcellular localization of the gene product were examined.

Molecular Characterization of the *CYP96A15* Gene and of T-DNA Insertional Mutant Lines

To test whether the *CYP96A15* gene is involved in wax biosynthesis, three T-DNA insertional mutants were obtained and characterized. Because we hypothesized that the corresponding gene product catalyzes a reaction introducing a hydroxyl group on a methylene unit in the middle of alkane molecules, we called the three mutant lines *mah1-1*, *mah1-2*, and *mah1-3* (for midchain alkane hydroxylase). Accordingly, the *CYP96A15* gene was tentatively designated as *MAH1*.

Initially, the wild-type *MAH1* gene was sequenced, corroborating previously published genomic information. Genomic DNA and cDNA templates gave identical full-length PCR products, thus confirming predictions that the *MAH1* gene does not contain any introns. To determine the nature and extent of gene disruption in the three T-DNA insertional lines, *MAH1* genomic regions were PCR amplified and sequenced. Sequencing confirmed the respective published T-DNA insert locations (Fig. 2A). Briefly, *mah1-1* plants had a T-DNA insertion within the coding region of the *MAH1* gene, 692 bp downstream from the translational start site; *mah1-2* plants were found to have a T-DNA insertion located in the 3′-untranslated region (UTR) of the gene, 1,601 bp downstream from the translational start site; and *mah1-3* plants contained a T-DNA insertion in the promoter region of the gene, 216 bp upstream of the translational start site. Semiquantitative reverse transcription (RT)-PCR assays using stem total RNA from these same mutants revealed normal *MAH1* steady-state transcript levels in *mah1-2*, reduced transcript levels in *mah1-3*, and truncated transcripts in *mah1-1* (Fig. 2B). All three mutant lines were observed to bolt and flower earlier than wild-type controls under the growth conditions used in this study.

Stem Cuticular Wax Phenotypes of *mah1* Mutants

To verify the involvement of *MAH1* in wax biosynthesis, cuticular wax on inflorescence stems of

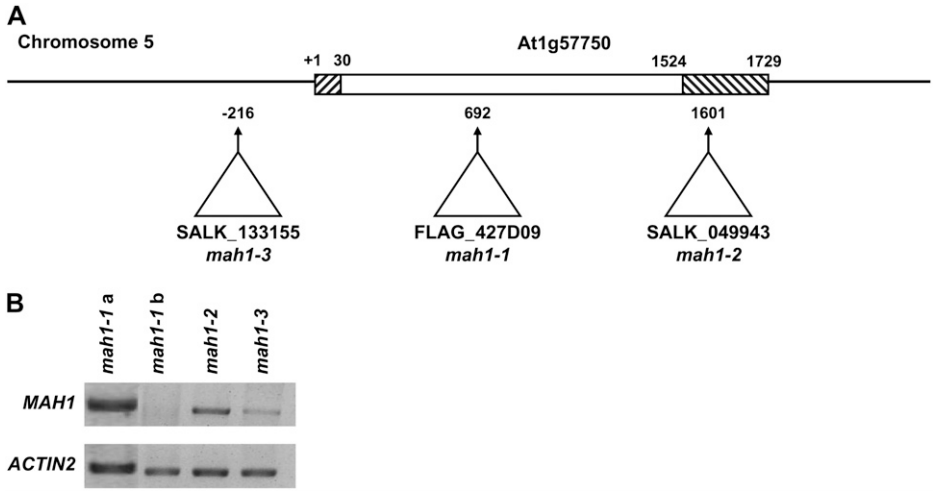

Figure 2. Structure of the *MAH1* gene and transcript levels in *mah1* mutant lines. A, Genomic organization of *MAH1* and location of T-DNA insertions in the mutant lines investigated here. The *MAH1* coding sequence is represented by a white box (there are no introns in At1g57750), the 3′-UTR sequence is indicated by diagonal hatching down and to the right, and the 5′-UTR sequence is indicated by diagonal hatching down and to the left. Arrows and numbers above them indicate the positions of the T-DNA insertions (triangles). B, Analysis of *MAH1* transcript levels in mutant stems. *MAH1* expression was analyzed by RT-PCR using total RNA and *ACTIN2* as a control. Two different sets of primers were employed to screen *mah1-1* to check for transcriptional knockout: Gene-specific results depicted in *mah1-1a* correspond to a unique set of primers ranging from the start site of the gene to approximately 60 bp upstream of the T-DNA insertion; *mah1-1b* results correspond to a set of primers spanning from 34 to 468 bp downstream of the insertion.

homozygous *mah1* mutant plants was analyzed and compared with the corresponding wild type. Only *mah1-3* plants were found to have total wax loads of 27 $\mu g/cm^2$, identical to the wild type (Table I). In contrast, *mah1-1* and *mah1-2* stems had wax coverages of 16 $\mu g/cm^2$ and 21 $\mu g/cm^2$, respectively, corresponding to approximately 40% and 15% reductions in wax amounts.

mah1-1 exhibited the most severe changes not only in overall wax amounts, but also in wax composition (Table I). Secondary alcohols and ketones were reduced from 2 $\mu g/cm^2$ and 6 $\mu g/cm^2$ in the wild type to 0.1 $\mu g/cm^2$ and < 0.05 $\mu g/cm^2$ in *mah1-1*, respectively, whereas the alkane fraction was found to be slightly increased from 10 $\mu g/cm^2$ in the wild type to 11 $\mu g/cm^2$ in the *mah1-1* mutant. Coverage of aldehydes, fatty acids, and primary alcohols was also reduced to some extent, whereas ester and triterpenoid amounts were similar to wild-type stem wax.

The other two mutants, *mah1-2* and *mah1-3*, also differed significantly from wild type in the levels of the major products of the decarbonylation pathway, whereas showing relatively small and mostly nonsignificant changes in the minor compound classes (Table I). *mah1-2* secondary alcohol and ketone levels were reduced to 71% and 25% of the wild-type loads, respectively, but these reductions were not as severe as those seen in *mah1-1*. At the same time, the *mah1-2* mutant also had alkane coverage increased above that of the wild type, with amounts similar to *mah1-1*.

Table I. *Cuticular wax composition of wild-type and mutant inflorescence stems*

Total wax amounts and coverage of individual compound classes ($\mu g/cm^2$) are given as mean values ± SE for individual compound classes ($n = 9$ in three batches). Different letters within the compound class show that wax loads differed significantly between respective lines (mixed-effect ANOVA; Tukey-Kramer posthoc test, $P < 0.05$). Trace and 0.0 signify values that were below 0.05 $\mu g/cm^2$. Mixed-effect ANOVA ($\alpha = 0.05$) was conducted using treatment as a fixed effect and batch nested within treatment as a random effect. Pertinent results for each compound class were as follows: Total load, F3, 8.132 = 11.083, $P = 0.003$, $\beta = 0.026$; alkanes, F3, 8.108 = 4.399, $P = 0.041$, $\beta = 0.337$; secondary alcohols, F3, 8.315 = 13.351, $P = 0.002$, $\beta = 0.009$; ketones, F3, 8.348 = 51.738, $P < 0.0005$, $\beta < 0.0005$; aldehydes, F3, 8.297 = 0.905, $P = 0.479$, $\beta = 0.827$; fatty acids, F3, 8.520 = 3.970, $P = 0.049$, $\beta = 0.374$; primary alcohols, F3, 8.141 = 1.899, $P = 0.207$, $\beta = 0.674$; esters, F3, 8.351 = 4.900, $P = 0.030$, $\beta = 0.280$; triterpenoids, F3, 8.185 = 2.475, $P = 0.134$, $\beta = 0.585$; not identified, F3, 8.241 = 1.686, $P = 0.244$, $\beta = 0.706$.

Line	Total Load	Alkanes	Secondary Alcohols	Ketones	Aldehydes	Fatty Acids	Primary Alcohols	Esters	Triterpenoids	Not Identified
Wild type (Col-0)	25.1 ± 0.6 a	9.6 ± 0.4 a	2.4 ± 0.1 a	6.0 ± 0.2 a	1.1 ± 0.2 a	0.4 ± 0.1 a	2.4 ± 0.3 a	1.0 ± 0.1 a	0.6 ± 0.1 a	1.8 ± 0.2 a
mah1-1	15.7 ± 1.0 b	11.2 ± 0.7 b	0.1 ± 0.0 b	Trace b	0.4 ± 0.1 b	0.1 ± 0.0 b	1.3 ± 0.1 b	0.9 ± 0.1 a	0.5 ± 0.1 a	1.2 ± 0.2 b
mah1-2	21.2 ± 0.6 c	11.8 ± 0.3 b	1.7 ± 0.1 c	1.5 ± 0.1 c	1.2 ± 0.2 a	0.4 ± 0.1 a	1.6 ± 0.3 b	0.9 ± 0.1 a	0.6 ± 0.1 a	1.4 ± 0.2 b
mah1-3	27.1 ± 1.1 a	13.7 ± 0.5 c	2.5 ± 0.1 a	3.2 ± 0.2 d	0.9 ± 0.2 ab	0.4 ± 0.1 a	2.4 ± 0.2 a	1.5 ± 0.2 b	0.8 ± 0.0 b	1.6 ± 0.2 ab

Although *mah1-3* had wild-type levels of secondary alcohols and the least severe ketone reduction (down to 53% of wild-type loads), this mutant had the highest accumulation of alkanes of all three mutant lines. The increase in alkane amounts within this mutant very nearly compensated for the reduction in ketones, resulting in an overall wax coverage similar to that of the wild type. The chain length patterns within wax compound classes were very similar for all three mutant lines (Fig. 3), showing dramatic increases of the C_{29} alkane over the wild-type level, whereas alkanes of other chain lengths were not affected. Taken together, the observed changes in the three major classes of stem wax compounds synthesized by the decarbonylation pathway in all three mutant lines clearly point to the involvement of *MAH1* in this branch of wax biosynthesis.

Remarkably, in spite of all the aforementioned quantitative (wax amounts) and qualitative (compositional) chemical variation between mutant and wild-type stem waxes, there were no discernible differences regarding the numbers, arrangement, size, or shape of epicuticular wax crystals on the stems (Supplemental Fig. S1).

Mutant Complementation and Ectopic Overexpression

To confirm the involvement of the *MAH1* gene in wax biosynthesis, MAH1 was expressed as a GFP fusion (MAH1:GFP) in the *mah1-1* mutant background under the control of either the native *MAH1* or the cauliflower mosaic virus (CaMV) 35S promoter. Multiple transgenic plants were analyzed and all were found to have significant restoration of the cuticular wax phenotype. Thin-layer chromatography (TLC) analyses of stem wax extracts showed a characteristic pattern of compound classes for the wild type from which *mah1-1* differed by the lack of secondary alcohols and ketones (Fig. 4). In contrast, stem wax from transgenics expressing *MAH1* (in the mutant background) showed a TLC pattern similar to wild type, containing secondary alcohols and ketones together with all other stem wax compound classes.

Further gas chromatography (GC) analyses revealed that a representative line expressing a C-terminal MAH1:GFP fusion under the control of the 35S promoter had stem wax containing ketones and secondary alcohols at 44% and 62% of wild-type levels, respectively; alkane coverage was found to be only 13% higher than in the wild type, thus well below the *mah1-1* levels (Table I). Similarly, the stem wax mixture of a line in which *MAH1* was expressed under the control of its native promoter contained ketones and secondary alcohols at approximately 30% and 77% of wild-type stem levels, respectively, and alkane coverage approximately 15% above wild type. Altogether, these results confirm that the mutant wax phenotypes

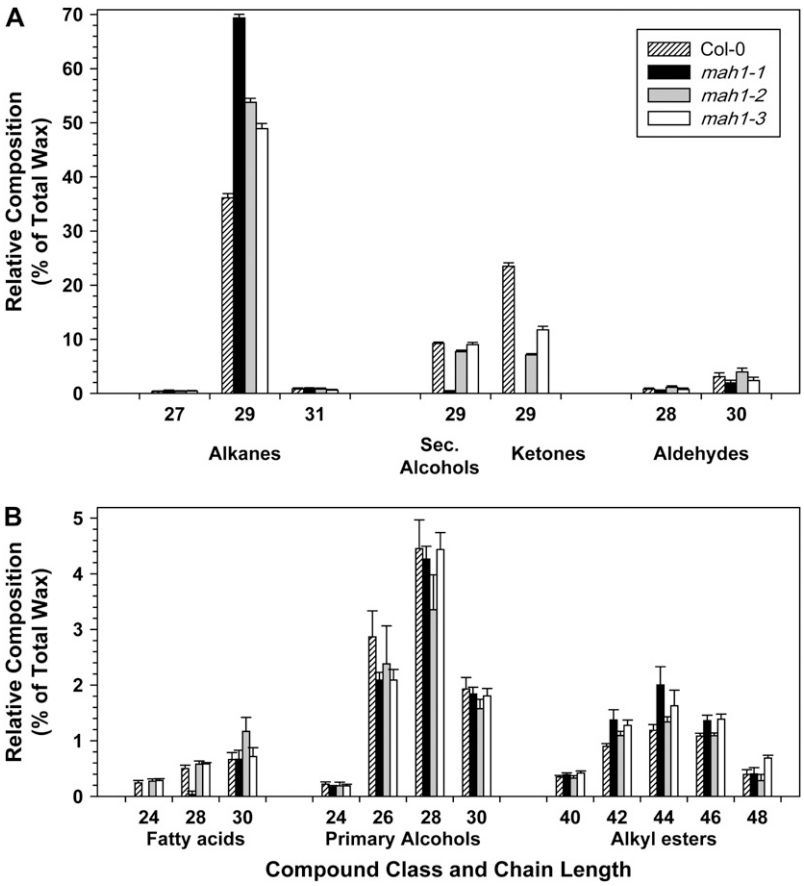

Figure 3. Chain length distributions within compound classes of cuticular wax on wild-type and *mah1* mutant stems. Compounds produced by the decarbonylation and acyl reduction pathways are shown in the top and bottom images, respectively. Data are expressed as mean percentages ± SE ($n = 9$) for individual compounds within the total wax mixture.

affecting products of the decarbonylation pathway are due to a defective *MAH1* gene.

Leaves of transgenic plants expressing MAH1-GFP under the control of the CaMV 35S promoter were used to further study biochemical activity of MAH1. Whereas alkanes dominated the leaf waxes of both the wild type and the *mah1* mutant, secondary alcohols and ketones could not be detected by TLC in either line (Fig. 4). Trace levels of the latter two compound classes could be identified by GC-mass spectrometry (MS) in wild-type leaf wax, but not in the mutant (data not shown). Thus, leaves represent an ideal tool for biochemical characterization of the MAH1 enzyme. *MAH1* was strongly expressed in leaves under the control of the CaMV 35S promoter (see Fig. 7F). TLC analysis showed that leaf wax of transgenics contained not only the characteristic wild-type wax constituents, but also substantial amounts of compound classes that coeluted with secondary alcohol and ketone standards (Fig. 4). The new leaf wax components were further studied by GC-MS and determined to be midchain secondary alcohols and ketones with functional groups either on or next to the central carbon of the chain, thus matching those found in stem wax (data not shown). Therefore, the results of ectopic expression confirm our hypothesis that *MAH1* (*CYP96A15*) codes for the enzyme catalyzing the conversion of wax alkane substrate into midchain alcohols and ketones and validate the gene's designation as *MAH1*. Further scanning electron microscopy (SEM) comparisons of leaves from transgenics expressing MAH1-GFP under the control of the CaMV 35S promoter and from *mah1-1* and wild-type controls revealed no morphological differences (cell shape or wax crystals) caused by the accumulation of these additional compounds (data not shown).

MAH1 Gene Expression Patterns

To investigate the expression patterns of the *MAH1* gene on the organ level, experiments using GUS fusion constructs and RT-PCR were performed. When expressed under the control of the native *MAH1* promoter in the wild-type background, GUS protein activity was found to be mainly present in nascent stems (Fig. 5A), petioles (Fig. 5, B and C), and developing siliques (Fig. 5, B, E, and F). Detailed analyses of stem expression revealed a pronounced gradient, where GUS activity was strongest in the upper 4 to 5 cm of the stem, still present in the next 10 to 12 cm, and conspicuously absent in stem regions more than 17 cm away from the meristem. Depending on the stage of development, floral organs also stained differentially for GUS, with nascent tissues exhibiting no staining (Fig. 5C) and older pistils revealing various levels of GUS activity (Fig. 5, D and E). Petals and sepals showed no GUS expression, with the exception of faint expression in the sepals of some older flowers (Fig. 5D). Under the same staining conditions, expression of GUS was absent from rosette leaves (data not shown), cauline leaves (Fig. 5A), seeds (Fig. 5F), and roots (Fig. 5G).

Stem-specific expression of *MAH1* was further verified by RT-PCR. Transcript levels of *MAH1* were found to be high in stems and flower buds of 4-week-old plants, whereas expression levels were relatively low (but consistently detectable) in roots and leaves (Fig. 6).

To further study *MAH1* expression in tissues within organs, the MAH1:GFP fusion construct under the control of the *MAH1* native promoter in *mah1-1* was employed. Stem cross sections revealed that *MAH1* expression was confined primarily to the layer of epidermal cells (Fig. 7A). MAH1-associated GFP fluorescence was localized in the pavement cells of the stem and petiole epidermis, but was absent from the guard cells and trichomes of these organs (Fig. 7, B and C). The same MAH1:GFP construct, when expressed under the control of the CaMV 35S promoter instead of the native promoter, was found in pavement cells as well as guard cells (Fig. 7D) and trichomes (data not shown) of the stem. This finding underscores that the native *MAH1* promoter alone causes the pavement cell-specific expression of this gene. Under the control of the native promoter, the fusion protein was only weakly expressed in some sepal tissues (Fig. 7B) and was absent from leaves (Fig. 7E). In contrast, intense

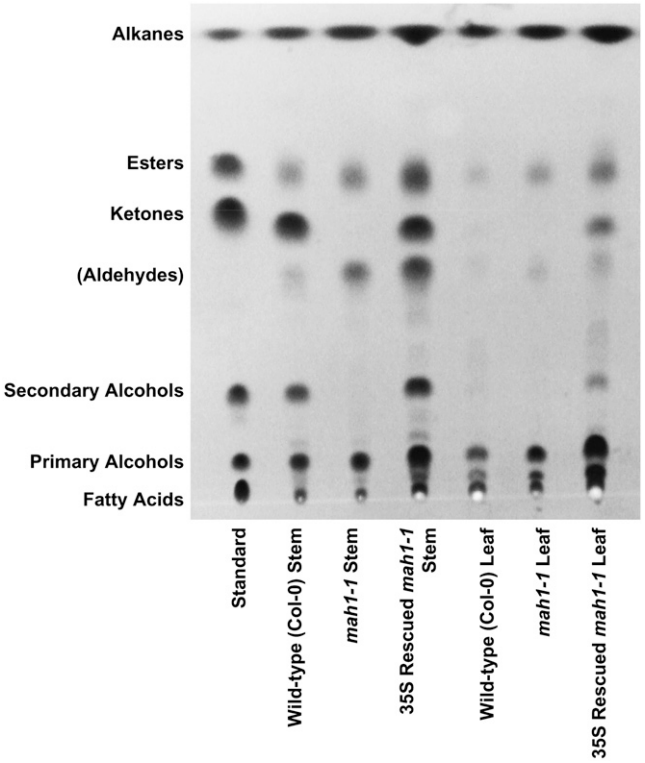

Figure 4. TLC analysis of wax mixtures from stems and leaves of Arabidopsis wild type, the *mah1-1* mutant line, and a transgenic line ectopically overexpressing *MAH1*. Compound classes are labeled on the left. The standard mixture was composed of tetracosanoic acid (fatty acid), heptacosanol (primary alcohol), nonacosan-11-ol (secondary alcohol), hentriacontan-16-one (ketone), docosyl eicosanoate (ester), and nonacosane (alkane). In the different lanes, wax extracts from wild-type, mutant, or transgenic stems and leaves were separated.

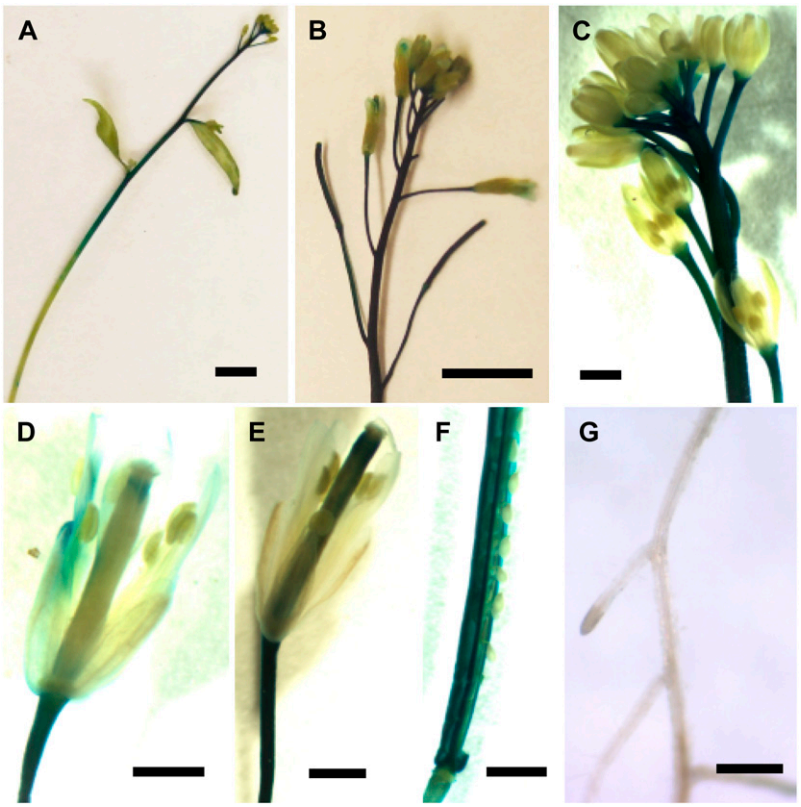

Figure 5. Organ expression patterns of *MAH1* detected in transgenic *MAH1*:GUS lines. Various organs of transgenic plants transformed with GUS reporter constructs expressed under control of the native promoter of *MAH1* are shown. Differential staining for GUS activity (blue) is indicative for organ-specific gene activity of *MAH1*. A to C, Top portions of inflorescence stems. D, Young flower. E, Mature flower. F, Mature silique. G, Root and root caps. Bars: A and B = 5 mm; C to F = 1 mm; G = 0.25 mm.

GFP fluorescence could be detected in pavement, guard, and trichome cells of transgenic leaves expressing the fusion driven by the 35S promoter (Fig. 7F).

Subcellular Localization of the *MAH1* Gene Product

GFP fusion constructs were also used to study the subcellular localization of the *MAH1* gene product and with it the site of the final steps in the decarbonylation pathway of wax biosynthesis. Under the control of either the native or the CaMV 35S promoters, GFP fluorescence in the stem epidermis of MAH1:GFP Arabidopsis transgenic lines was most intense within reticulate networks typical of the endoplasmic reticulum (ER; Fig. 8). Subsequent treatment with rhodamine B hexyl ester, a dye capable of staining the ER, confirmed ER localization of the MAH1 protein (Supplemental Fig. S2). When expressed under the control of the 35S promoter, MAH1 fusion protein was also localized in the ER of Arabidopsis leaf epidermal cells. Transient expression of CaMV 35S-expressed MAH1:GFP in wild-type tobacco (*Nicotiana tabacum*) leaves also displayed a subcellular pattern akin to that observed in *mah1-1* plants (data not shown).

DISCUSSION

The principal goal of this study was to identify and characterize a gene encoding a wax biosynthesis enzyme involved in the decarbonylation pathway. We chose the cytochrome P450 gene *CYP96A15* as a primary candidate and hypothesized that the corresponding enzyme catalyzes the oxidation reactions yielding the secondary alcohols and ketones that accumulate in the stem wax of Arabidopsis.

MAH1 (CYP96A15) Is a Midchain Alkane Hydroxylase Involved in the Formation of Secondary Alcohols and Ketones in Arabidopsis Stems

Several allelic T-DNA insertion mutants of the *MAH1* (*CYP96A15*) gene all showed cuticular wax phenotypes, with secondary alcohols and ketones either missing entirely or present in significantly smaller quantities than on the wild-type stem. Wax of the mutant lines also contained alkanes in higher relative (% of total wax) and absolute ($\mu g/cm^2$) amounts than

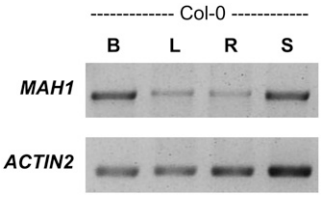

Figure 6. Organ expression patterns of *MAH1* detected by RT-PCR analysis of native *MAH1* transcript in Col-0 wild-type organs. Gene-specific primers (identical to those used for *mah1-1b* in Fig. 2) were used to screen flower buds (B), leaves (L), roots (R), and stems (S).

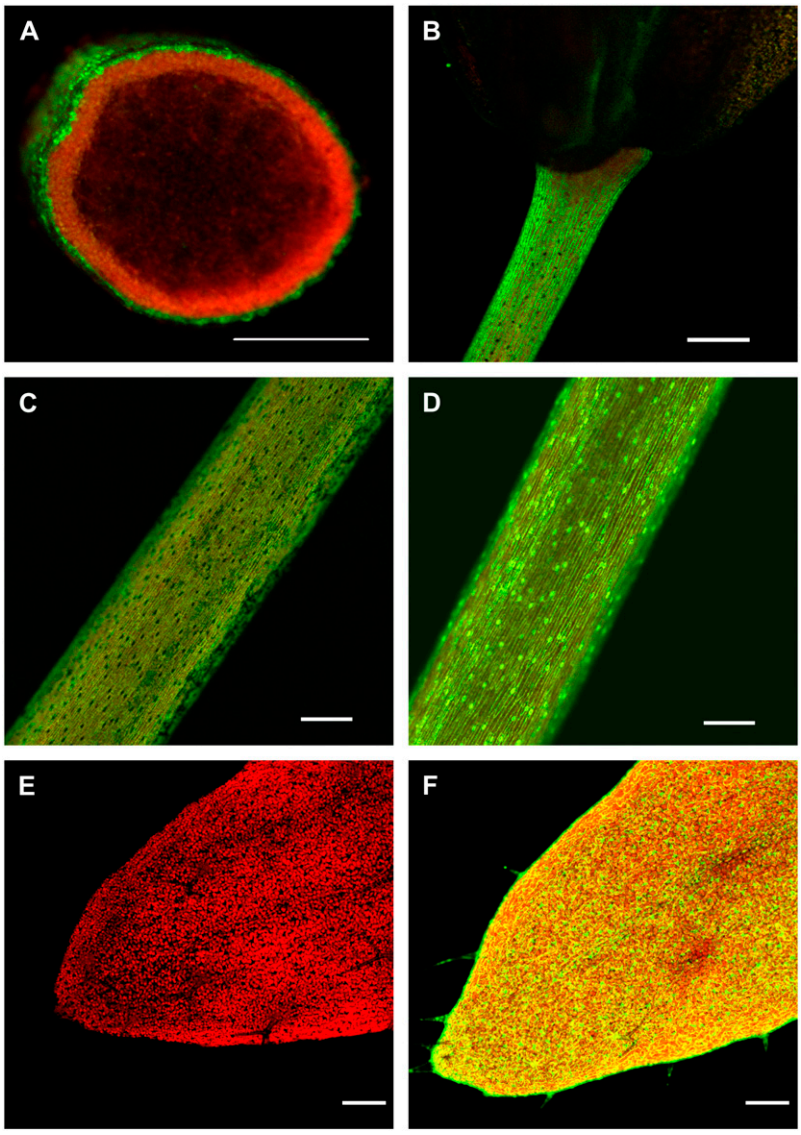

Figure 7. Tissue expression patterns of *MAH1* detected in transgenic MAH1:GFP lines. MAH1:GFP fusion protein expressed in the *mah1-1* mutant background under the control of the native promoter was visualized (in conjunction with autofluorescence depicted as red in the images) in stems, petioles, sepals, and leaves (A, B, C, and E). MAH1:GFP fusion protein expressed in the *mah1-1* mutant background under the control of the CaMV 35S promoter was analyzed in stems (D) and leaves (F). All images are layered (autofluorescence and GFP) signals. All bars = 200 μm.

the wild type, which in turn partially or fully compensated for the loss of secondary alcohols and ketones. Other changes in mutant wax composition were relatively minor. Secondary alcohol and ketone deficiencies were partially rescued by expression of *MAH1* under the control of either the native promoter or the CaMV 35S promoter. Taken together, these results clearly show that the cytochrome P450 enzyme encoded by *MAH1* (*CYP96A15*) is involved in the formation of wax secondary alcohols and ketones.

In combination with previous reports in the literature, our results can be used to specifically define substrates utilized by the CYP96A15 enzyme. Prior studies had demonstrated that exogenous nonacosane (C_{29} alkane) is incorporated into secondary alcohols and ketones by *B. oleracea* leaves (Kolattukudy and Liu, 1970; Kolattukudy et al., 1973). As a result, alkane is assumed to be the in vivo substrate for the hydroxylation reactions in the wax biosynthetic pathway yielding secondary alcohols and ketones (Fig. 1; Kolattukudy, 1996; Rashotte et al., 2001; Jenks et al., 2002). However, because these biosynthetic steps had not been confirmed to date, the alternative scenario could not be ruled out that acyl or aldehyde precursors may also be hydroxylated and the resulting hydroxyacids or hydroxyaldehydes transformed into secondary alcohols (Kunst et al., 2006). According to this hypothesis, hydroxylation would occur before decarbonylation and secondary alcohols and alkanes would be formed as parallel, rather than direct, sequential products in the pathway. However, none of the hydroxylated intermediate products that would be produced by this alternative scenario (in particular, hydroxyaldehydes) have been reported in Arabidopsis cuticular lipids to date. Our finding that reduced levels of secondary alcohols and ketones occur in tandem with increased levels of alkanes also points to a direct precursor-product relationship between these compound

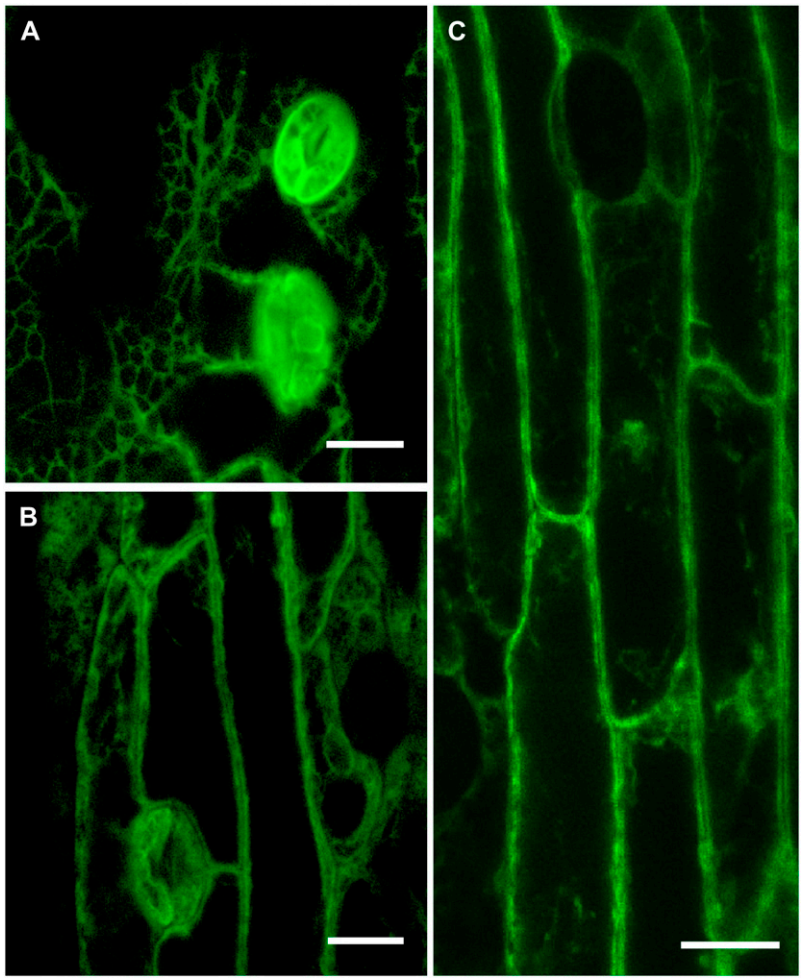

Figure 8. Subcellular localization of MAH1:GFP expression. MAH1:GFP fusion protein expressed in the *mah1-1* mutant background under the control of the CaMV 35S promoter was visualized in leaves (A) and stems (B). MAH1:GFP fusion protein expressed in the *mah1-1* mutant background under the control of the native promoter was visualized in stems (C). All bars = 10 μm.

classes, arguing further against aldehyde or acid hydroxylation. Thus, it appears most likely that the CYP96A15 enzyme functions as an alkane hydroxylase.

Ectopic expression of MAH1 in Arabidopsis leaves led to the formation of secondary alcohols and ketones with chain lengths and isomer compositions matching those on wild-type stems. This result, together with the absence of those compounds in *mah1* mutants, shows that the enzyme is specifically hydroxylating the central carbons of its alkane substrates, thus confirming its designation as a midchain alkane hydroxylase. To our knowledge, this is the first alkane hydroxylase reported from plants. Only few such enzymes had previously been described in bacteria and yeast (*Saccharomyces cerevisiae*; van Beilen et al., 2003; van Beilen and Funhoff, 2007) and only a few of these are able to metabolize medium- to long-chain alkane ($\leq C_{16}$) substrates. Furthermore, among the few long-chain alkane hydroxylases that have been successfully cloned and characterized, none are reported to be cytochrome P450 enzymes (Tani et al., 2001; van Beilen and Funhoff, 2007).

MAH1 (CYP96A15) is currently classified as a member of the CYP86 clan of non-A-type P450 enzymes, most of which are thought to use fatty acids as substrates (Nelson et al., 2004). The biochemical action of MAH1 is quite unique because it is able to hydroxylate long-chain alkanes in the center of the molecule (midchain). This distinguishes it from most other known P450 enzymes, alkane hydroxylases, and fatty acid hydroxylases, which can only catalyze reactions on terminal or subterminal carbons of the substrates (e.g. ω-1 or ω-2; Whyte et al., 1998; van Beilen et al., 2003; Kandel et al., 2005, 2006). To date, only one other P450 enzyme with in-chain hydroxylase activity has been described and it prefers C12 fatty acid substrates very different from the VLC alkane substrates of MAH1 (Morant et al., 2007). The ability of *MAH1* to catalyze midchain alkane hydroxylation suggests a unique active-site morphology for this enzyme, a unique folding of the alkane substrate, or perhaps a combination of these two conditions.

Current gene ontology classifies MAH1 as a eukaryotic-type P450 enzyme (Mulder et al., 2007). Based on its sequence, the protein is predicted to have a hydrophobic transmembrane (Transmembrane Hidden Markov Model, version 2; Sonnhammer et al., 1998) N-terminal signal anchor (0.903 probability using

SignalP 3.0 with defaults; Bendtsen et al., 2004; Emanuelsson et al., 2007) with secretory/ER targeting (TargetP 1.1 = 0.970; WoLF PSORT = 5.0 with defaults; Nakai and Horton, 1999; Bendtsen et al., 2004; Emanuelsson et al., 2007). Our subcellular localization results confirm these bioinformatic predictions. E-type class II P450 enzymes associated with the ER most frequently have a cluster of Pros (Pro-Pro-X-Pro) preceded by a cluster of basic residues (the halt-transfer signal) between the hydrophobic amino-terminal membrane-anchoring segment and the globular part of the protein (Werck-Reichhart and Feyereisen, 2000); curiously, MAH1 possesses such a Pro-rich ER-targeting region, but it is located in the middle of the protein primary sequence at position 365 to 369 of the 497-amino acid protein. It should be noted that MAH1 also contains a group I domain similar to some other P450 enzymes and proteins of diverse other families.

MAH1 Is Involved in Secondary Alcohol and Ketone Biosynthesis

The reaction sequence leading from alkanes to secondary alcohols and ketones involves two distinct steps that might be catalyzed either by the same cytochrome P450 or by two separate enzymes, with at least the first of them being a cytochrome P450. This raises the question of whether one or both of these steps are catalyzed by MAH1 in Arabidopsis. Regarding the first reaction, the stem wax of *mah1-1* mutants was found to lack not only the ketone end products of the pathway, but also the secondary alcohol intermediates. Furthermore, the ectopic expression of MAH1 in Arabidopsis leaves led to the formation of secondary alcohols above the levels found in wild-type wax. These results both unambiguously show that the enzyme must be involved in the initial hydroxylation transforming alkanes into secondary alcohols.

Our ectopic expression data also provide information on whether MAH1 further catalyzes the second oxidation from secondary alcohols to ketones. Expression of MAH1 in the leaf epidermis led to the accumulation of ketones (together with secondary alcohols) well above the trace amounts found in the leaf wax of the wild type. The appearance of ketones may be due to (1) MAH1 carrying out both steps of the reaction sequence; (2) a specific leaf enzyme being dedicated to this step; or (3) an unspecific enzyme catalyzing the further oxidation of secondary alcohols in the leaf.

The existence of a leaf enzyme capable of oxidizing wax secondary alcohols to ketones might explain the low levels of ketones that have been reported for the waxes of the Landsberg *erecta* and Wassilewskija wild-type leaves (Rashotte et al., 1997, 2001) and found here for the Columbia (Col) wild type. However, it is important to note that both new products accumulated in the transgenic leaf wax in a ratio similar to that on the wild-type stem, making it unlikely that a nonspecific leaf enzyme catalyzed the second reaction while MAH1 carried out the first step (scenario 3).

The second oxidation (secondary alcohols to ketones) can be likened to the initial step (alkanes to secondary alcohols) if both reactions are described as hydroxylations occurring on the same carbon atom of the two substrates. The second hydroxylation then transforms an alcohol (-CHOH-) into a geminal diol (-$C(OH)_2$-) that will be spontaneously dehydrated into the final ketone (-CO-) product. Both reactions are thus very similar, each replacing one hydrogen atom of the methylene unit by an OH group. Therefore, it seems plausible that a single enzyme, capable of carrying out hydroxylations on the central carbon, should catalyze both consecutive reactions leading from alkanes to secondary alcohols and on to ketones. This hypothesis argues against the presence of a specific enzyme carrying out the second oxidation reaction in the leaves, with MAH1 catalyzing only the first step (scenario 2).

Further evidence against scenario 2 is provided by a comparison between the secondary alcohol and ketone amounts in the stem waxes of wild type and the *mah1-2* and *mah1-3* lines. If the two reactions were carried out by two independent enzymes, then the second enzyme should have slightly lower activity than (approximately 75% of) the first one (MAH1) to account for the 1:3 ratio of secondary alcohols to ketones in the wild type. Consequently, *mah1* mutations affecting only the first step of the sequence should reduce secondary alcohol levels much more than ketone levels. In stark contrast to this scenario, all the *mah1* mutants have more severely reduced ketone than secondary alcohol levels. The *mah1-3* mutant can serve as an extreme example where secondary alcohol levels are identical to the wild type, whereas ketone levels are reduced by approximately 50%. Of all the above arguments, we favor the hypothesis that MAH1 acts both as an alkane hydroxylase and as a secondary alcohol hydroxylase (scenario 1).

The double activity of MAH1 is reminiscent of a few other cytochrome P450 enzymes that also oxidize hydrocarbons to ketones (Turnbull et al., 2004; Jungmann et al., 2005; Ortiz de Montellano and De Voss, 2005). However, possible double activity of MAH1 would differ from these ketone-forming enzymes because it produces a characteristic mixture of ketone and secondary alcohol products. This mixture occurred at various MAH1 enzyme levels, both in wild-type leaves with weak expression of the *MAH1* gene and in leaves ectopically expressing it at high levels. These results are in good accordance with the hypothesis that MAH1 catalyzes the second reaction step (scenario 1); however, they do not provide sufficient proof for it at this point.

The evidence that MAH1 is the enzyme required for formation of wax secondary alcohols and ketones in the stem wax of wild-type Arabidopsis sheds new light on other gene products that had previously been implied in late steps of the decarbonylation pathway. Most notably, *cer20* stems had been found to show lower levels of secondary alcohols and ketones than

the wild type (Rashotte et al., 2001; Jenks et al., 2002), thus resembling *mah1* stem wax. Based on this phenotype, it had been suggested that CER20 might be an enzyme responsible for the midchain oxidation of alkanes. However, our work on MAH1 indicates that the involvement of other enzymes in the process is unlikely. *CER20* and *MAH1* are different genes located on Arabidopsis chromosomes 5 and 1, respectively, and therefore *CER20* must have a nonenzymatic function affecting secondary alcohol and ketone accumulation. It may be speculated that *CER20* codes for a protein associated with MAH1 (e.g. through redox coupling), a protein involved in wax secretion, or a regulator of the decarbonylation pathway. In this context, it might be interesting to note that the *cer20* stem wax contained alkane amounts similar to the wild type, thus differing from the *mah1* phenotype with its increased alkane concentration.

The varying total amounts of decarbonylation pathway products (alkanes, secondary alcohols, and ketones together) in *mah1* mutants suggest that some form of feedback inhibition is occurring. Severe losses of ketone and secondary alcohol products were associated with significant increases in alkane amounts in all mutant lines, but only within a range of 11 to 14 $\mu g/cm^2$. Further reductions in the ketone and secondary alcohol levels resulted in decreases in total wax loads rather than more alkane accumulation. In all of these cases, other metabolites upstream from alkane formation in the wax pathways did not change in similar proportion to changes of ketone, secondary alcohol, and total wax loads. Overall, these results indicate that accumulation of alkanes to a characteristic threshold level prompts the down-regulation of upstream reactions in wax biosynthetic pathways.

Loss of MAH1 Activity and Its Secondary Alcohol and Ketone Products Does Not Affect Epicuticular Wax Crystals on Arabidopsis Stems

An interesting finding of this study is that all the *mah1* mutant lines had glaucous inflorescence stems indistinguishable from the wild type. Even the *mah1-1* allele, with the most severely reduced *MAH1* transcript levels leading to a complete absence of secondary alcohols and ketones in the stem wax, showed visually normal surfaces. This result explains why previous visual screens for wax mutants with glossy stems had not yielded any candidate lines with defects in the *MAH1* gene.

The glaucous appearance of *mah1* stems prompted us to further investigate the epicuticular wax crystals on these mutant cuticles with SEM. The stem surfaces of all three mutant lines were covered with similar numbers of wax crystals as the wild type and the crystal shapes were also indistinguishable from those on the wild type. These findings are noteworthy because alkanes, secondary alcohols, and ketones had all been implicated in the formation of wax crystals on Arabidopsis stem surfaces (Rashotte and Feldmann, 1998; Jetter et al., 2006) and changes in the amounts of these compounds in the (total) wax mixture might therefore be expected to affect the appearance of the epicuticular wax crystals. To understand why the surface structures instead appeared unaltered in the mutants, the exact composition of wild-type and mutant crystals will have to be assessed directly.

Final Steps of the Decarbonylation Pathway Are Localized in the ER of Epidermal Pavement Cells of the Arabidopsis Inflorescence Stem

We found that *MAH1* is expressed most strongly in the inflorescence stems, petioles, and siliques, but not weakly in the rosette and cauline leaves, seeds, and roots of Arabidopsis. These results are in agreement with published predictions for gene expression (Zimmermann et al., 2004). *MAH1* expression was found to be restricted to the epidermal layer of stems, again confirming previous predictions based on microarray data (Suh et al., 2005). Finally, *MAH1* gene activity was highest in the actively growing parts of the inflorescence stems in the same regions where rapid cuticle formation occurs. Chemical analyses had shown that this is also the part of the plant surface where secondary alcohols and ketones accumulate most rapidly (Suh et al., 2005), whereas they are almost absent from the leaf wax (Jenks et al., 2002). Based on the perfect correlation between expression patterns and metabolite occurrence, it can be concluded that MAH1 functions mainly, or even exclusively, as a hydroxylase in the decarbonylation pathway of stem wax biosynthesis.

MAH1 expression was limited to the pavement cells of the stem epidermis, whereas it was absent from guard cells (and trichomes). Based on this finding, it can be expected that the wax composition of these types of epidermal cells will differ at least in the amounts of secondary alcohols and ketones. It is currently not known whether the different types of Arabidopsis stem epidermal cells are also autonomous in the expression of other genes involved in cuticle formation, possibly causing further differences in their surface compositions. In this context, it is interesting to note that guard cells lacked the epicuticular wax crystals typical for the pavement cells of wild-type and *mah1* mutant stems (data not shown). Hence, both epidermal cell types differ in surface composition and structure, creating a heterogeneous surface patchwork that will, in turn, cause locally varying properties and affect the biological functions of the Arabidopsis stem surface.

On a subcellular level, MAH1 was confined to the ER of stem epidermal cells. This localization of the enzyme implies that the final steps of the decarbonylation pathway occur in this compartment and that alkanes, secondary alcohols, and ketones are likely present at substantial concentrations in the ER membranes during biosynthesis. The current results thus define the subcellular compartment where all the

major cuticular wax components are being generated, including intermediates and end products. It follows that the wax metabolites must be picked up in the ER for transport to the plasma membrane from which ATP-binding cassette transporters are thought to export them toward the cuticle (Pighin et al., 2004; Bird et al., 2007). Even though intracellular trafficking of wax molecules is crucial for successful cuticle formation, and hence for plant survival, nothing is known about the mechanisms involved. The current data at least allow us to pinpoint the starting location of wax trafficking within the cell and might consequently help future studies into its mechanism.

CONCLUSION

We have identified and characterized the Arabidopsis cytochrome P450 enzyme CYP96A15 and found it to function as a unique midchain alkane hydroxylase (MAH1). The enzyme was demonstrated to be involved in two consecutive steps of the decarbonylation pathway of cuticular wax biosynthesis, catalyzing the hydroxylation of alkanes to secondary alcohols and possibly also to ketones. Interestingly, neither reduced concentrations nor a total loss of secondary alcohols and ketones in *mah1* mutant lines affected the appearance of epicuticular wax crystals on the stems. *MAH1* was expressed predominantly in epidermal pavement cells (but not guard cells) of inflorescence stems, and the MAH1 enzyme was localized to the ER of the epidermis cells. Because all wax biosynthetic enzymes identified and studied to date have been localized to the ER, it seems likely that the entire process of wax biosynthesis is confined to a single subcellular compartment. This hypothesis leads to the prediction that subcellular trafficking must start with all the wax products in the ER and transport mechanisms must be operating that shunt the metabolites to the plasma membrane and on to the cuticle.

MATERIALS AND METHODS

Plant Material

The T-DNA insertional mutant line *mah1-1* (flanking sequence tag no. 427D09; Samson et al., 2002) was obtained from the Institut National de la Recherche Agronomique. T-DNA insertional mutant lines *mah1-2* (SALK_049943) and *mah1-3* (SALK_133155; Alonso et al., 2003) were obtained from the Arabidopsis Biological Resource Center. Seeds from all lines were initially planted and screened for allele homozygosity using genomic DNA extraction from leaves (Berendzen et al., 2005) and touchdown PCR (Don et al., 1991). Primers for screening and sequencing were designed with the aid of sequence-indexed Arabidopsis (*Arabidopsis thaliana*) T-DNA insertion data supplied by the Salk Institute for Genomic Analysis Web sites (http://signal.salk.edu/cgi-bin/tdnaexpress and http://signal.salk.edu/isects.html). Locations of reported insertion sites were confirmed by direct sequencing of flanking PCR products (utilizing a left-border T-DNA-specific forward primer in conjunction with a gene-specific reverse primer). Seeds from the positively identified homozygous lines were used to grow plants for all subsequent experiments.

Seeds were spread upon Arabidopsis agar plates (Somerville and Ogren, 1982) with 5 mM KNO_3, 2.5 mM KH_2PO_4, 2 mM $MgSO_4$, $7H_2O$, 2 mM $Ca(NO_3)_2$, $4H_2O$, 50 μM Fe(EDTA), 70 μM H_3BO_3, 14 μM $MnCl_2$, $4H_2O$, 10 μM NaCl, 1 μM $ZnSO_4$, $7H_2O$, 0.2 μM $NaMoO_4$, $2H_2O$, 0.05 μM $CuSO_4$, 0.01 μM $CoCl_2$, $6H_2O$, 0.8% agar, pH adjusted to 5.6 with KOH, and then stratified for 2 to 4 d at 4°C. Plates were placed under continuous light (approximately 150 μmol m^{-2} s^{-1} photosynthetically active radiation) for 7 to 10 d at 21°C for germination. Young seedlings were then transplanted into soil (1:1 ratio of Sunshine Mix 5 [SunGro Horticulture] and Seeding Mix [West Creek Farms]) and grown under the same light and temperature conditions as above.

Wax Extraction and Chemical Characterization

Leaves or stems were harvested from plants 4 to 7 weeks after plating. Total cuticular wax mixtures were extracted by immersing whole organs twice for 30 s into chloroform ($CHCl_3$). The two solutions were combined, *n*-tetracosane (C_{24} alkane) was added as an internal standard, and the solvent was completely evaporated under vacuum. In TLC analyses, approximately 2 mg of wax were separated on silica gel with chloroform mobile phase using the sandwich technique (Tantisewie et al., 1969) and visualized by staining with primuline and UV light.

For GC analyses, samples were resuspended in approximately 300 μL of $CHCl_3$, transferred to a GC autosampler vial, dried under nitrogen, and derivatized with 10 μL of *N*,*O*-bis(trimethylsilyl) trifluoroacetamide (Sigma) and 10 μL pyridine (Fluka) for 60 min at 70°C. Wax composition was analyzed using a capillary GC (5890 N; Agilent; column 30-m HP-1, 0.32-mm i.d., d_f = 0.1 μm; Agilent) with He carrier gas inlet pressure programmed for constant flow of 1.4 mL min^{-1} with a MS detector (5973 N; Agilent). GC was carried out with temperature-programmed on-column injection and oven temperature set at 50°C for 2 min, raised by 40°C min^{-1} to 200°C, held for 2 min at 200°C, raised by 3°C min^{-1} to 320°C, and held for 30 min at 320°C. Individual wax components were identified by comparing their mass spectra with those of authentic standards and literature data. Quantitative analysis of wax mixtures was carried out using capillary GC with flame ionization detector under the same conditions as above, but with H_2 carrier gas inlet pressure regulated for constant flow of 2 mL min^{-1}.

Wax loads were determined by comparing GC-flame ionization detector peak areas against internal standard and dividing by the surface area extracted for the corresponding sample. Total leaf surface areas were calculated with ImageJ software (Abramoff et al., 2004) by measuring the apparent leaf areas in digital photographs and multiplying by 2. Stem surface areas were calculated by measuring the projected two-dimensional stem areas in photographs and multiplying by π.

Semiquantitative RT-PCR

Total RNA was extracted from stems, roots, buds, and leaves of 4-week-old plants grown in soil. Tissues were ground up thoroughly in 200 μL of RNA later (Ambion/Applied Biosystems), using a tube and motorized pestle. The lysate was processed immediately by a Qiagen RNeasy plant mini kit and then used as template for RT by Moloney murine leukemia virus reverse transcriptase (New England Biolabs). cDNAs used for semiquantitative RT-PCR were normalized based on the intensity of PCR-amplified *ACTIN2* fragments generated by the primers 5′-CCAGAAGGATGCATATGTTGGTGA-3′ and 5′-GAGGAGCCTCGGTAAGAAGA-3′ (yielding an approximately 250-bp fragment). *MAH1* gene-specific primers 5′-AACTTTGTGCCCGCTTGGAA-3′ and 5′-ACAGCTTTGGCCACTGTCAA-3′ (generating a 434-bp fragment) were used in reactions conducted simultaneously under identical conditions as *ACTIN2* controls. Because these primers amplify a downstream region of the gene stretching from +726 to +1,160 and because the *mah1-1* T-DNA insert had been proposed to be localized approximately at position +692, we used an additional set of primers, 5′-ATGGCGATGCTAGGTTTTTACGTA-3′ and 5′-TTCGCCAATATCCGCAGCTT-3′ ranging from +1 to +638 to determine *mah1-1* steady-state transcript levels.

Cryo-SEM

Segments from the apical 4 to 6 cm of stems were mounted onto cryo-SEM stubs using graphite paste and plunged into liquid nitrogen. Frozen stems were transferred into an Emitech K1250 cryosystem and water sublimed for 10 min at −110°C. Samples were viewed with a Hitachi S4700 field emission SEM (Nissei Sangyo America) using an accelerating voltage of 1.5 kV and a working distance of 12 mm.

Cloning of *MAH1* and Construction of Vectors for Expression of MAH1:GFP and *MAH1* Promoter:GUS Fusions

With aid from The Arabidopsis Information Resource SeqViewer (http://www.arabidopsis.org), 3,126 bp of Arabidopsis chromosome 1 surrounding and including the At1g57750 coding sequence (GenBank accession no. AY090941) was PCR amplified (Phusion DNA pol; Finnzymes/NEB) using isolated genomic Col-0 DNA as a template with primers 5′-GCCGTTGGATGATGAATATGCACGACT-3′ and 5′-TTACAAAGATTCGAGGACCGGGCA-3′. The resulting product included the proposed 5′-UTR, 3′-UTR, the entire open reading frame (which lacks introns) of *MAH1* (*CYP96A15*), and the additional nucleotide sequence stretching 1,310 bp upstream of the 5′-UTR. This genomic fragment was cloned into pGEM-EZ (Promega), then sequenced and found to perfectly match The Institute for Genomic Research sequence published on The Arabidopsis Information Resource. All subsequent constructs were made by using this clone as template.

Two MAH1-GFP C-terminal fusion constructs were produced using GATEWAY λ-phage-based site-specific recombination (Landy, 1989; Hartley et al., 2000; Walhout et al., 2000). The first, pGWB4-MAH1N (the pGWB series was a kind gift from Tsuyoshi Nakagawa, Shimane University; all pGWB sequences are available at http://bio2.ipc.shimane-u.ac.jp/pgwbs/index.htm), was designed to express MAH1:GFP under the control of the native (approximately 1,310 bp) promoter and the second, pGWB5-MAH135S, was designed to express MAH1:GFP under the control of the CaMV 35S promoter. pGWB4-MAH1N was constructed using the forward primer 5′-GGGGACAAGTTTGTACAAAAAAGCAGGCTTTGCCGTTGGATGATGAATATGCACGACT-3′ (underlined sequences = directional *att*B sites) and the reverse primer (without a stop codon) 5′-GGGGACCACTTTGTACAAGAAAGCTGGGTTTATCTTCTTTGTGACTGTGACTTTAAGACC-3′. pGWB5-MAH135S was constructed using the forward primer 5′-GGGGACAAGTTTGTACAAAAAAGCAGGCTTTATGGCGATGCTAGGTTTTTACGTA-3′ along with the same reverse primer as pGWB4-MAH1N. One *MAH1* promoter:GUS fusion construct (pGWB3-MAH1P) was produced by using the reverse primer 5′-GGGGACCACTTTGTACAAGAAAGCTGGGTCAAAAGGATTTATGAGTATAGATACAAAACT-3′ (spanning into the 5′-UTR) along with the forward primer from pGWB4-MAH1N.

Resultant PCR products were placed into vector pDONR221 (Invitrogen) by performing a BP reaction (*att*B × *att*P → *att*L + *att*R) using Integrase and Integration Host Factor in the form of BP Clonase II (Invitrogen). Integrated constructs were then inserted in frame into binary vectors for fusion with either GFP (pGWB4 or pGWB5) or GUS (pGWB3) by performing an *att*L × *att*R → *att*B + *att*P reaction (LR reaction with Integrase, Integration Host Factor, and excisionase in the form of LR Clonase II from Invitrogen) between the entry clone (pDONR221) and the appropriate pGWB acceptor vector. Finished binary vector constructs were sequenced to confirm that the sequence was maintained.

GUS and GFP Visualization

Expression of GUS in transgenic pGWB3-MAH1P:GUS wild-type (Col-0) plants was assayed by submerging whole-plant tissues in acetone under vacuum for 30 min and then washing in buffer composed of 0.1% Triton X-100, 0.25 mM $K_4Fe(CN)_6$, $3H_2O$, 0.25 mM $K_3Fe(CN)_6$, $3H_2O$, and 50 mM phosphate buffer, pH 7.0, three times for 5 min each. Washed tissues were subsequently stained by incubation in this same buffer with the addition of 1 mM 5-bromo-4-chloro-3-indolyl-β-D-glucuronide under vacuum for 30 min, and then at ambient pressure (with gentle agitation) at 37°C for 16 h. Afterward, stained tissues were placed in 70% ethanol and imaged using a Stemi 2000-C dissecting microscope (Zeiss) mounted with a QCAM digital camera (QImaging) and Openlab 4.01 software (Improvision).

Arabidopsis plants were immersed for 10 to 30 min either in FM4-64 (8.2 μM) solution (Vida and Emr, 1995) for plasma membrane staining or in rhodamine B hexyl ester solution (1.6 μM) for ER staining. Autofluorescence, as well as GFP, rhodamine B hexyl ester, and FM4-64 fluorescence was examined with a Zeiss LSM 5 Pascal confocal laser-scanning microscope. The excitation wavelength for GFP was 488 nm with the emission filter set at 505 to 530 nm; autofluorescence was detected using an emission filter set at 600 to 650 nm. The excitation wavelength for rhodamine B hexyl ester was 568 nm with the emission filter set at 600 to 650 nm. The excitation wavelength for FM4-64 was 514 nm with the emission filter set at 600 to 650 nm.

Statistics

Comparisons of wild-type and mutant wax data utilizing mixed-effect univariate ANOVA ($\alpha = 0.05$; treatment as a fixed effect, batch nested within treatment as a random effect), Dunnett's *t*, and Tukey-Kramer posthoc tests ($\alpha = 0.05$; using harmonic means in cases of unequal *n*) were conducted with SPSS 11.0 software. When necessary to meet assumptions of normality or equal variance, datasets were transformed into normal scores using Tukey's formula $(r - 1/3)/(w + 1/3)$, where *r* is the rank and *w* is the sum of the case weights (Tukey, 1962). For each analysis, type II error statistics (β) were also calculated. Values for β range from 0 to 1 and correspond directly to the chance of committing type II error in an ANOVA *F* test. The power of an ANOVA *F* test can be calculated as $1 - \beta$, yielding the probability that the *F* test will detect the differences between groups equal to those implied by sample differences (Sokal and Rohlf, 1995).

Supplemental Data

The following materials are available in the online version of this article.

Supplemental Figure S1. Cryo-SEM of inflorescence stem surfaces.

Supplemental Figure S2. Confirmation of MAH1 subcellular localization.

ACKNOWLEDGMENTS

We thank the Salk Institute for Genomic Analysis Laboratory for providing sequence-indexed Arabidopsis T-DNA insertion mutants, Tsuyoshi Nakagawa for the pGWB vector series, and John Shin and the Bioimaging Facility at the University of British Columbia for providing microscopy and technical support.

Received August 13, 2007; accepted September 20, 2007; published September 28, 2007.

LITERATURE CITED

Aarts MGM, Keijzer CJ, Stiekema WJ, Pereira A (1995) Molecular characterization of the *CER1* gene of Arabidopsis involved in epicuticular wax biosynthesis and pollen fertility. Plant Cell **7:** 2115–2127

Abramoff MD, Magelhaes PJ, Ram SJ (2004) Image processing with ImageJ. Biophotonics International **11:** 36–42

Alonso JM, Stepanova AN, Leisse TJ, Kim CJ, Chen H, Shinn P, Stevenson DK, Zimmerman J, Barajas P, Cheuk R, et al (2003) Genome-wide insertional mutagenesis of *Arabidopsis thaliana.* Science **301:** 653–657

Barthlott W, Neinhuis C (1997) Purity of the sacred lotus, or escape from contamination in biological surfaces. Planta **202:** 1–8

Bendtsen JD, Nielsen H, von Heijne G, Brunak S (2004) Improved prediction of signal peptides: SignalP 3.0. J Mol Biol **340:** 783–795

Berendzen K, Searle I, Ravenscroft D, Koncz C, Batschauer A, Coupland G, Somssich I, Ulker B (2005) A rapid and versatile combined DNA/RNA extraction protocol and its application to the analysis of a novel DNA marker set polymorphic between *Arabidopsis thaliana* ecotypes Col-0 and Landsberg erecta. Plant Methods **1:** 4

Bird D, Beisson F, Brigham A, Shin J, Greer S, Jetter R, Kunst L, Wu X, Yephremov A, Samuels L (August 28, 2007) Characterization of Arabidopsis *WBC11/ABCG11*, an ATP binding cassette (ABC) transporter that is required for cuticular lipid secretion. Plant J http://dx.doi.org/10.1111/j.1365-313X.2007.03252.x

Burghardt M, Riederer M (2006) Cuticular transpiration. *In* M Riederer, C Müller, eds, Annual Plant Reviews 23: Biology of the Plant Cuticle. Blackwell, Oxford, pp 292–311

Carver TLW, Gurr SJ (2006) Filamentous fungi on plant surfaces. *In* M Riederer, C Müller, eds, Annual Plant Reviews 23: Biology of the Plant Cuticle. Blackwell, Oxford, pp 368–397

Chen X, Goodwin SM, Liu X, Chen X, Bressan RA, Jenks MA (2005) Mutation of the *RESURRECTION1* locus of Arabidopsis reveals an association of cuticular wax with embryo development. Plant Physiol **139:** 909–919

Collu G, Garcia AA, van der Heijden R, Verpoorte R (2002) Activity of the cytochrome P450 enzyme geraniol 10-hydroxylase and alkaloid production in plant cell cultures. Plant Sci **162:** 165–172

Collu G, Unver N, Peltenburg-Looman AM, van der Heijden R, Verpoorte R, Memelink J (2001) Geraniol 10-hydroxylase, a cytochrome P450 enzyme involved in terpenoid indole alkaloid biosynthesis. FEBS Lett **508:** 215–220

Don RH, Cox PT, Wainwright BJ, Baker K, Mattick JS (1991) Touchdown PCR to circumvent spurious priming during gene amplification. Nucleic Acids Res **19:** 4008

Durst F, Nelson DR (1995) Diversity and evolution of plant P450 and P450-reductases. Drug Metabol Drug Interact **12:** 189–206

Ehlting J, Hamberger B, Million-Rousseau R, Werck-Reichhart D (2006) Cytochromes P450 in phenolic metabolism. Phytochem Rev **5:** 239–270

Eigenbrode SD, Espelie KE (1995) Effects of plant epicuticular lipids on insect herbivores. Annu Rev Entomol **40:** 171–194

Emanuelsson O, Brunak S, von Heijne G, Nielsen H (2007) Locating proteins in the cell using TargetP, SignalP and related tools. Nat Protocols **2:** 953–971

Fiebig A, Mayfield JA, Miley NL, Chau S, Fischer RL, Preuss D (2000) Alterations in *CER6*, a gene identical to *CUT1*, differentially affect long-chain lipid content on the surface of pollen and stems. Plant Cell **12:** 2001–2008

Hartley JL, Temple GF, Brasch MA (2000) DNA cloning using in vitro site-specific recombination. Genome Res **10:** 1788–1795

Hooker TS, Millar AA, Kunst L (2002) Significance of the expression of the CER6 condensing enzyme for cuticular wax production in Arabidopsis. Plant Physiol **129:** 1568–1580

Jeffree CE (2006) The fine structure of the plant cuticle. *In* M Riederer, C Müller, eds, Annual Plant Reviews 23: Biology of the Plant Cuticle. Blackwell, Oxford, pp 11–125

Jenks MA, Eigenbrode SD, Lemieux B (2002) Cuticular waxes of Arabidopsis. *In* CR Somerville, EM Meyerowitz, eds, The Arabidopsis Book. American Society of Plant Biologists, Rockville, MD

Jetter R, Kunst L, Samuels AL (2006) Composition of plant cuticular waxes. *In* M Riederer, C Müller, eds, Annual Plant Reviews 23: Biology of the Plant Cuticle. Blackwell, Oxford, pp 145–181

Jungmann V, Molnar I, Hammer PE, Hill DS, Zirkle R, Buckel TG, Buckel D, Ligon JM, Pachlatko JP (2005) Biocatalytic conversion of avermectin to 4′′-oxo-avermectin: characterization of biocatalytically active bacterial strains and of cytochrome P450 monooxygenase enzymes and their genes. Appl Environ Microbiol **71:** 6968–6976

Kahn RA, Le Bouquin R, Pinot F, Benveniste I, Durst F (2001) A conservative amino acid substitution alters the regiospecificity of CYP94A2, a fatty acid hydroxylase from the plant *Vicia sativa*. Arch Biochem Biophys **391:** 180–187

Kandel S, Morant M, Benveniste I, Blee E, Werck-Reichhart D, Pinot F (2005) Cloning, functional expression, and characterization of CYP709C1, the first sub-terminal hydroxylase of long chain fatty acid in plants: induction by chemicals and methyl jasmonate. J Biol Chem **280:** 35881–35889

Kandel S, Sauveplane V, Olry A, Diss L, Benveniste I, Pinot F (2006) Cytochrome P450-dependent fatty acid hydroxylases in plants. Phytochem Rev **5:** 359–372

Kim HB, Schaller H, Goh CH, Kwon M, Choe S, An CS, Durst F, Feldmann KA, Feyereisen R (2005) Arabidopsis *cyp51* mutant shows postembryonic seedling lethality associated with lack of membrane integrity. Plant Physiol **138:** 2033–2047

Kolattukudy PE (1996) Biosynthetic pathways of cutin and waxes, and their sensitivity to environmental stresses. *In* G Kerstiens, ed, Plant Cuticles: An Integrated Functional Approach. BIOS Scientific, Oxford, pp 83–108

Kolattukudy PE, Buckner JS, Liu TY (1973) Biosynthesis of secondary alcohols and ketones from alkanes. Arch Biochem Biophys **156:** 613–620

Kolattukudy PE, Jaeger RH, Robinson R (1971) Biogenesis of nonacosan-15-one in *Brassica oleracea*. Phytochemistry **10:** 3047–3051

Kolattukudy PE, Liu TY (1970) Direct evidence for biosynthetic relationships among hydrocarbons, secondary alcohols, and ketones in *Brassica oleracea*. Biochem Biophys Res Commun **41:** 1369–1374

Koornneef M, Hanhart CJ, Thiel F (1989) A genetic and phenotypic description of *eceriferum* (*cer*) mutants in *Arabidopsis thaliana*. J Hered **80:** 118–122

Krauss P, Markstädter C, Riederer M (1997) Attenuation of UV radiation by plant cuticles from woody species. Plant Cell Environ **20:** 1079–1085

Kunst L, Jetter R, Samuels AL (2006) Biosynthesis and transport of plant cuticular waxes. *In* M Riederer, C Müller, eds, Annual Plant Reviews 23: Biology of the Plant Cuticle. Blackwell, Oxford, pp 182–215

Landy A (1989) Dynamic, structural, and regulatory aspects of lambda site-specific recombination. Annu Rev Biochem **58:** 913–941

Leveau JHJ (2006) Microbial communities in the phyllosphere. *In* M Riederer, C Müller, eds, Annual Plant Reviews 23: Biology of the Plant Cuticle. Blackwell, Oxford, pp 334–367

Mau C, Croteau R (2006) Cytochrome P450 oxygenases of monoterpene metabolism. Phytochem Rev **5:** 373–383

McNevin JP, Woodward W, Hannoufa A, Feldmann KA, Lemieux B (1993) Isolation and characterization of *eceriferum* (*cer*) mutants induced by T-DNA insertions in *Arabidopsis thaliana*. Genome **36:** 610–618

Millar AA, Clemens S, Zachgo S, Giblin EM, Taylor DC, Kunst L (1999) *CUT1*, an Arabidopsis gene required for cuticular wax biosynthesis and pollen fertility, encodes a very-long-chain fatty acid condensing enzyme. Plant Cell **11:** 825–838

Morant M, Jorgensen K, Schaller H, Pinot F, Moller BL, Werck-Reichhart D, Bak S (2007) CYP703 is an ancient cytochrome P450 in land plants catalyzing in-chain hydroxylation of lauric acid to provide building blocks for sporopollenin synthesis in pollen. Plant Cell **19:** 1473–1487

Morikawa T, Mizutani M, Aoki N, Watanabe B, Saga H, Saito S, Oikawa A, Suzuki H, Sakurai N, Shibata D, et al (2006) Cytochrome P450 *CYP710A* encodes the sterol C-22 desaturase in *Arabidopsis* and tomato. Plant Cell **18:** 1008–1022

Mulder NJ, Apweiler R, Attwood TK, Bairoch A, Bateman A, Binns D, Bork P, Buillard V, Cerutti L, Copley R, et al (2007) New developments in the InterPro database. Nucleic Acids Res **35:** D224–228

Müller C (2006) Plant-insect interactions on cuticular surfaces. *In* M Riederer, C Müller, eds, Annual Plant Reviews 23: Biology of the Plant Cuticle. Blackwell, Oxford, pp 398–422

Nakai K, Horton P (1999) PSORT: a program for detecting sorting signals in proteins and predicting their subcellular localization. Trends Biochem Sci **24:** 34–36

Nawrath C (2006) Unraveling the complex network of cuticular structure and function. Curr Opin Plant Biol **9:** 281–287

Nelson DR, Schuler MA, Paquette SM, Werck-Reichhart D, Bak S (2004) Comparative genomics of rice and Arabidopsis: analysis of 727 cytochrome P450 genes and pseudogenes from a monocot and a dicot. Plant Physiol **135:** 756–772

Ortiz de Montellano PR, De Voss JJ (2005) Substrate oxidation by P450 enzymes. *In* PR Ortiz de Montellano, ed, Cytochrome P450: Structure, Mechanism, and Biochemistry, Ed 3. Kluwer Academic/Plenum, New York, pp 183–245

Pfündel EE, Agati G, Cerovic ZG (2006) Optical properties of plant surfaces. *In* M Riederer, C Müller, eds, Annual Plant Reviews 23: Biology of the Plant Cuticle. Blackwell, Oxford, pp 216–249

Pighin JA, Zheng H, Balakshin LJ, Goodman IP, Western TL, Jetter R, Kunst L, Samuels AL (2004) Plant cuticular lipid export requires an ABC transporter. Science **306:** 702–704

Rashotte AM, Feldmann KA (1998) Correlations between epicuticular wax structures and chemical composition in *Arabidopsis thaliana*. Int J Plant Sci **159:** 773–779

Rashotte AM, Jenks MA, Feldmann KA (2001) Cuticular waxes on *eceriferum* mutants of *Arabidopsis thaliana*. Phytochemistry **57:** 115–123

Rashotte AM, Jenks MA, Nguyen TD, Feldmann KA (1997) Epicuticular wax variation in ecotypes of *Arabidopsis thaliana*. Phytochemistry **45:** 251–255

Rhee SY, Beavis W, Berardini TZ, Chen G, Dixon D, Doyle A, Garcia-Hernandez M, Huala E, Lander G, Montoya M, et al (2003) The Arabidopsis Information Resource (TAIR): a model organism database providing a centralized, curated gateway to Arabidopsis biology, research materials and community. Nucleic Acids Res **31:** 224–228

Rowland O, Lee R, Franke R, Schreiber L, Kunst L (2007) The *CER3* gene from *Arabidopsis thaliana* is allelic to WAX2/YRE/FLP1 and is required for cuticular wax biosynthesis. FEBS Lett **581:** 3538–3544

Rowland O, Zheng H, Hepworth SR, Lam P, Jetter R, Kunst L (2006) *CER4* encodes an alcohol-forming fatty acyl-coenzyme A reductase involved in cuticular wax production in Arabidopsis. Plant Physiol **142:** 866–877

Samson F, Brunaud V, Balzergue S, Dubreucq B, Lepiniec L, Pelletier G, Caboche M, Lecharny A (2002) FLAGdb/FST: a database of mapped flanking insertion sites (FSTs) of *Arabidopsis thaliana* T-DNA transformants. Nucleic Acids Res **30:** 94–97

Sokal RR, Rohlf FJ (1995) Biometry: The Principles and Practice of Statistics in Biological Research, Ed 3. Freeman, New York

Solovchenko A, Merzlyak M (2003) Optical properties and contribution of cuticle to UV protection in plants: experiments with apple fruit. Photochem Photobiol Sci **2:** 861–866

Somerville CR, Ogren WL (1982) Isolation of photorespiratory mutants of Arabidopsis. *In* RB Hallick, NH Chua, eds, Methods in Chloroplast Molecular Biology. Elsevier, New York, pp 129–139

Sonnhammer EL, von Heijne G, Krogh A (1998) A hidden Markov model for predicting transmembrane helices in protein sequences. Proc Int Conf Intell Syst Mol Biol **6:** 175–182

Suh MC, Samuels AL, Jetter R, Kunst L, Pollard M, Ohlrogge J, Beisson F (2005) Cuticular lipid composition, surface structure, and gene expression in Arabidopsis stem epidermis. Plant Physiol **139:** 1649–1665

Tani A, Ishige T, Sakai Y, Kato N (2001) Gene structures and regulation of the alkane hydroxylase complex in *Acinetobacter* sp. strain M-1. J Bacteriol **183:** 1819–1823

Tantisewie B, Ruijgriok HWL, Hegnauer R (1969) Die verbreitung der blausäure bei den kormophyten. Pharm Weekbl **104:** 1341–1355

Tukey JW (1962) The future of data analysis. Ann Math Stat **33:** 1–67

Turnbull JJ, Nakajima JI, Welford RWD, Yamazaki M, Saito K, Schofield CJ (2004) Mechanistic studies on three 2-oxoglutarate-dependent oxygenases of flavonoid biosynthesis: anthocyanidin synthase, flavonol synthase, and flavanone 3β-hydroxylase. J Biol Chem **279:** 1206–1216

van Beilen JB, Funhoff E (2007) Alkane hydroxylases involved in microbial alkane degradation. Appl Microbiol Biotechnol **74:** 13–21

van Beilen JB, Li Z, Duetz WA, Smits THM, Witholt B (2003) Diversity of alkane hydroxylase systems in the environment. Oil and Gas Science and Technology **58:** 427–440

Vida TA, Emr SD (1995) A new vital stain for visualizing vacuolar membrane dynamics and endocytosis in yeast. J Cell Biol **128:** 779–792

Walhout A, Temple G, Brasch M, Hartley J, Lorson M, van den Heuvel S, Vidal M (2000) GATEWAY recombinational cloning: application to the cloning of large numbers of open reading frames or ORFeomes. Methods Enzymol **328:** 575–592

Wellesen K, Durst F, Pinot F, Benveniste I, Nettesheim K, Wisman E, Steiner-Lange S, Saedler H, Yephremov A (2001) Functional analysis of the *LACERATA* gene of Arabidopsis provides evidence for different roles of fatty acid omega-hydroxylation in development. Proc Natl Acad Sci USA **98:** 9694–9699

Werck-Reichhart D, Bak S, Paquette S (2002) Cytochromes P450. *In* CR Somerville, EM Meyerowitz, eds, The Arabidopsis Book. American Society of Plant Biologists, Rockville, MD

Werck-Reichhart D, Feyereisen R (2000) Cytochromes P450: a success story. Genome Biol **1:** 1–8

Whitbred JM, Schuler MA (2000) Molecular characterization of *CYP73A9* and *CYP82A1* P450 genes involved in plant defense in pea. Plant Physiol **124:** 47–58

Whyte LG, Hawari J, Zhou E, Bourbonniere L, Inniss WE, Greer CW (1998) Biodegradation of variable-chain-length alkanes at low temperatures by a psychrotrophic *Rhodococcus* sp. Appl Environ Microbiol **64:** 2578–2584

Wortman JR, Haas BJ, Hannick LI, Smith RK, Maiti R, Ronning CM, Chan AP, Yu C, Ayele M, Whitelaw CA, et al (2003) Annotation of the Arabidopsis genome. Plant Physiol **132:** 461–468

Zheng H, Rowland O, Kunst L (2005) Disruptions of the *Arabidopsis* enoyl-CoA reductase gene reveal an essential role for very-long-chain fatty acid synthesis in cell expansion during plant morphogenesis. Plant Cell **17:** 1467–1481

Zimmermann P, Hirsch-Hoffmann M, Hennig L, Gruissem W (2004) GENEVESTIGATOR: Arabidopsis microarray database and analysis toolbox. Plant Physiol **136:** 2621–2632